J Solid State Electrochem (2012) 16:391–402
DOI 10.1007/s10008-011-1330-y

ORIGINAL PAPER

Corrosion inhibitive properties and electrochemical adsorption behaviour of some piperidine derivatives on brass in natural sea water

Joseph Raj Xavier · Rajendran Nallaiyan

Received: 7 October 2010 / Revised: 13 January 2011 / Accepted: 5 February 2011 / Published online: 6 April 2011

Abstract The piperidine derivatives, namely (4-Hydrazono-2,6-diphenyl-piperidin-1-yl)-ethanoic acid hydrazide; 5-(2,6-diphenyl-4-hydrazono-piperidin-1-ylmethyl)-3H-[1, 3, 4]oxadiazole-2-thione; 4-amino-5-(2,6-diphenyl-4-hydrazono-piperidin-1-ylmethyl)-4H-[1, 2, 4] triazole-3-thiol were synthesised and characterised by Fourier transform-infrared spectroscopic studies to confirm the purity of compounds. The corrosion inhibition effect of these compounds on brass in natural sea water was studied using potentiodynamic polarisation studies and electrochemical impedance spectroscopic measurements. The presence of these inhibitors in sea water suppresses both anodic and cathodic processes, and it is enhanced by the increase in the concentration of the inhibitors. The surface morphology of the brass after its exposure to natural sea water with and without inhibitors was examined by scanning electron microscopy. Inductively Coupled Plasma Atomic Emission Spectroscopic analysis were carried out after the polarisation studies showed minimum leached out of metal ions from the brass specimen in the presence of inhibitors. The structural and electronic parameters of these piperidine derivatives were calculated using computational methodologies.

Keywords Brass · Corrosion inhibitors · Polarisation · EIS · SEM-EDX

J. R. Xavier · R. Nallaiyan (✉)
Department of Chemistry, Anna University,
Chennai 600 025, India
e-mail: nrajendran@annauniv.edu

Introduction

Copper and its alloys exhibit high electrical and thermal conductivity, high formability, machinability and strength, hence they are extensively used as a material in heating and cooling systems, potable water pipes, valves, heat exchanger tubes, wire, screens, shafts, roofing, bearings, stills, tanks and printed circuits. Brass has been widely used for shipboard condensers, power plant condensers and petrochemical heat exchangers [1–3]. These materials also have good corrosion resistance to acids as well as chloride-containing media [4–7]. Dezincification of brass is one of the well-known and common processes by means of which brass loses its valuable physical and mechanical properties leading to structural failure. Organic compounds containing an azole nucleus have been found effective inhibitors for copper alloys in a variety of aggressive environments [8].

Many organic compounds, especially those containing polar groups and/or substituted heterocycle including nitrogen, sulphur and oxygen in their structures, have been reported to inhibit the corrosion of copper [9–11]. The inhibiting action of these organic compounds is usually attributed to the formation of donor–acceptor surface complexes between the free or π electrons of an inhibitor and the vacant *d*-orbital of a metal and adsorption [12] and to their molecular structure [13]. Recently, it has been shown that the adsorption of organic inhibitors mainly depends on physicochemical and electronic properties of the molecule, related to their functional groups, steric effects, electron density of donor atoms and the π orbital character of donating electrons [14, 15]. We have already carried out extensive studies on the corrosion of brass in sea water using benzotriazole derivatives [16]. However, the literature reports indicated that the piperidine derivatives are strong complexing agents for transition metal ions [17].

The objective of the work is to investigate the inhibition effect of some piperidine derivatives, namely (4-Hydrazono-2,6-diphenyl-piperidin-1-yl)-ethanoic acid hydrazide (HDPEH); 5-(2,6-diphenyl-4-hydrazono-piperidin-1-ylmethyl)-3H-[1, 3, 4]oxadiazole-2-thione (DHPOT); 4-amino-5-(2,6-diphenyl-4-hydrazono-piperidin-1-ylmethyl)-4H-[1, 2, 4]triazole-3-thiol (ADHPTT) on the corrosion of brass in natural sea water.

Experimental section

Synthesis of corrosion inhibitors

A schematic route of the synthesis of the organic compound tested as corrosion inhibitor was shown in Fig. 1. The chemicals were analytical grade and used as purchased without further purifications.

HDPEH was prepared by the following procedure. A solution of (4-oxo-2,6–diphenyl-piperidin-1-yl)-ethanoic acid (12.36 g, 0.04 M) and hydrazine hydrochloric acid (4.00 g, 0.08 M) in ethanol (100 ml) was taken in a three-necked flask equipped with a refluxing condenser, thermometer and a dropping funnel. The reaction mixture was refluxed over a hot water bath for 3 h with continuous stirring. The contents were cooled and poured into crushed ice. The precipitate obtained was filtered, washed with water and recrystallised from absolute alcohol. The yield was 13.72 g (70%).

DHPOT was synthesised by reacting a mixture of (4-hydrazono-2,6-diphenyl-piperidin-1-yl)-ethanoic acid hydrazide (3.37 g, 0.01 M) in ethanol (200 ml), with a solution of KOH (0.84 g, 0.015 M) in ethanol (20 ml) and CS_2 (20 ml). The reaction mixture was heated under reflux for 8 h. Then it was concentrated, acidified with dilute hydrochloric acid and the resulting solid was collected, washed with water and

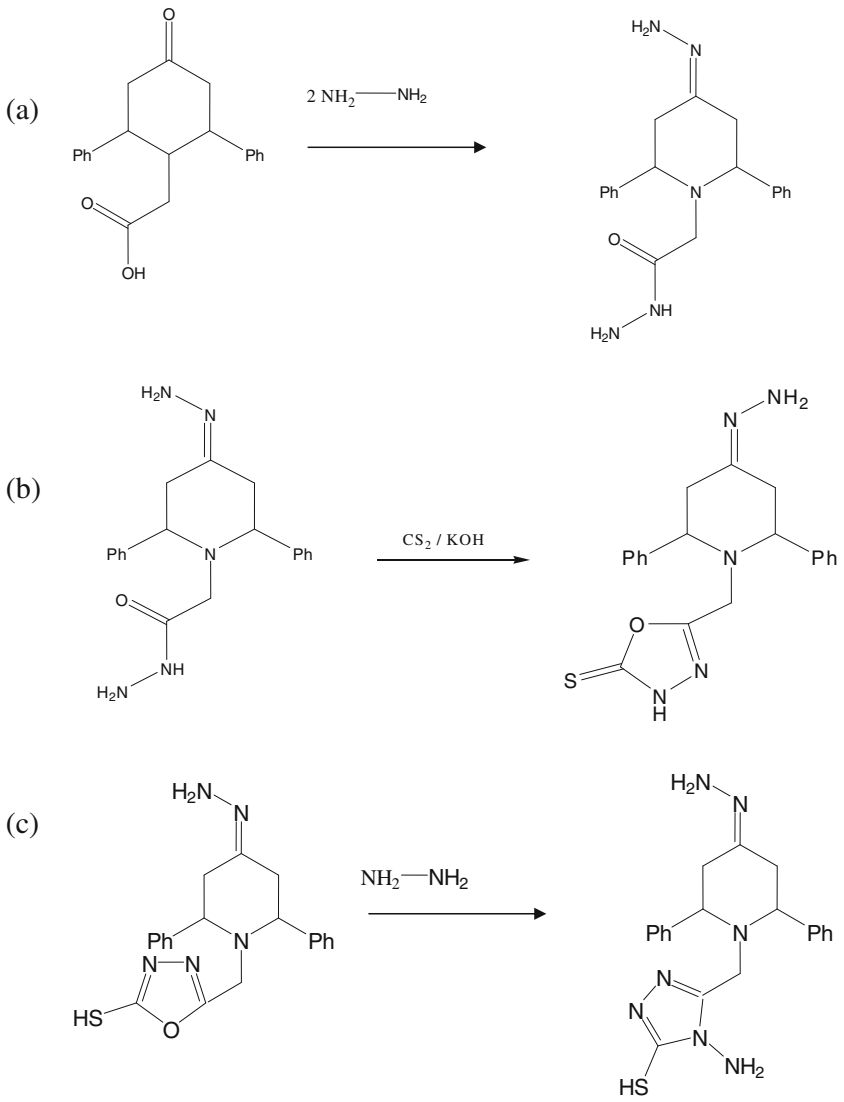

Fig. 1 The synthetic route of piperidine derivatives **a** HDPEH, **b** DHPOT and **c** ADHPTT

recrystallised from petroleum ether to give the product. The product yield was 81%.

ADHPTT was prepared by refluxing a mixture of 5-(2,6-diphenyl-4-hydrazono-piperidin-1-ylmethyl)-3H-[1, 3, 4] oxadiazole-2-thione (3.79 g, 0.01 M) and 99% hydrazine hydrate (2 ml, 0.03 M) in absolute ethanol (20 ml) for 6 h. The solvent and the excess hydrazine hydrate were removed under reduced pressure, the residue was washed with ether, then recrystallised from petroleum ether to give the product. The product yield was 71%. These products were characterised by FT-IR, ^{1}H nuclear magnetic resonance spectroscopy and microanalysis methods.

Materials

The electrolyte used was the natural sea water collected in a sterilised brown flask at Elliott beach on the southern coast of Chennai, India. The working electrode used for the study having the chemical composition as weight (percent) 65.3 Cu, 34.44 Zn, 0.1385 Fe and 0.0635 Sn. The brass specimens were polished mechanically with different grades of silicon carbide papers (400–1,200) and washed with double-distilled water. Further, the samples were degreased with acetone using ultrasonicator and thoroughly washed with double-distilled water and dried in air. Different concentrations of the inhibitors were added into the electrolyte to find out the optimum concentration of the inhibitor.

Potentiodynamic polarisation studies

An electrochemical cell with a three-electrode assembly was used to study the electrochemical measurements. Brass specimens with exposed area of 0.28 cm^2, a platinum foil of 1 cm^2 area and silver–silver chloride Ag/AgCl in saturated KCl (Advance-Tech Controls Pvt. Ltd, India) were used as working, counter and reference electrodes respectively. The polarisation experiments were carried out using the Potentiostat/Galvanostat (model PGSTAT 12, Autolab, The Netherlands B.V.) controlled by a personal computer with dedicated software (GPES version 4.9.005). The working electrode was immersed in natural sea water in the presence and absence of different concentrations of the inhibitors to which a current of −1.0 mA cm^{-2} was applied for 15 min to reduce oxides and then allowed to stabilise for 30 min [18]. The polarisation experiments were carried out for brass specimen at a scan rate of 1 mV/s in the presence and absence of inhibitors in natural sea water. In order to test the reproducibility of the results, the experiments were performed in triplicate.

Electrochemical impedance spectroscopy

Electrochemical impedance spectroscopy (EIS) measurements were conducted using a potentiostat/galvanostat (model PGSTAT 12, Autolab, (ECO CHEMIE B.V. Netherlands) The Netherlands B.V.) with frequency response analyzer. The impedance measurements were carried out at an open-circuit potential, after 30 min immersion of the brass electrode in the corrosive medium. The impedance data were acquired in the frequency range of 100–50 mHz with an AC voltage amplitude of 10 mV.

Inductively coupled plasma atomic emission spectroscopy

The concentration of copper and zinc in the electrolytes, after the polarisation experiments in the presence and absence of 10^{-3} M piperidine derivatives, were determined by Inductively Coupled Plasma Atomic Emission Spectroscopy (ICP-AES). An ICP-AES (ARCOS from Spectro, Germany) was used to measure the amount of dissolution of zinc and copper from the brass surface. The dezincification factor (z) was calculated using the equation [19],

$$z = \frac{\left[C_{\mathrm{Zn}/}C_{\mathrm{Cu}}\right]\mathrm{sol}}{\left[C_{\mathrm{Zn}/}C_{\mathrm{Cu}}\right]\mathrm{alloy}} \quad (1)$$

where, $[C_{\mathrm{Zn}}/C_{\mathrm{Cu}}]_{\mathrm{sol}}$ and $[C_{\mathrm{Zn}}/C_{\mathrm{Cu}}]_{\mathrm{alloy}}$ are the ratios between the concentrations of zinc and copper in the solution and in the alloy respectively.

SEM and EDX investigations

The brass surface was prepared by keeping the specimens for an hour in the electrolyte with and without the optimum concentrations of the inhibitors. The brass specimens were then washed with distilled water, dried and analysed using scanning electron microscopy (SEM)/energy dispersive x-ray analysis (EDX). A Philips model XL30SFEG scanning electron microscope with an energy dispersive X-ray analyser attached was used for surface analysis.

Results and discussion

Potentiodynamic polarisation measurements

Polarisation measurements were performed for brass specimens in natural sea water in the absence and presence of various concentrations of the inhibitors, HDPEH, DHPOT and ADHPTT; the obtained results are presented in Fig. 2. It can be seen that both the cathodic and anodic curves are influenced by the presence of inhibitors and the effect depends on the concentration and molecular structure of the inhibitors. The addition of piperidine derivatives gives rise to significant decrease in cathodic and anodic current densities as compared to the blank solution which indicates

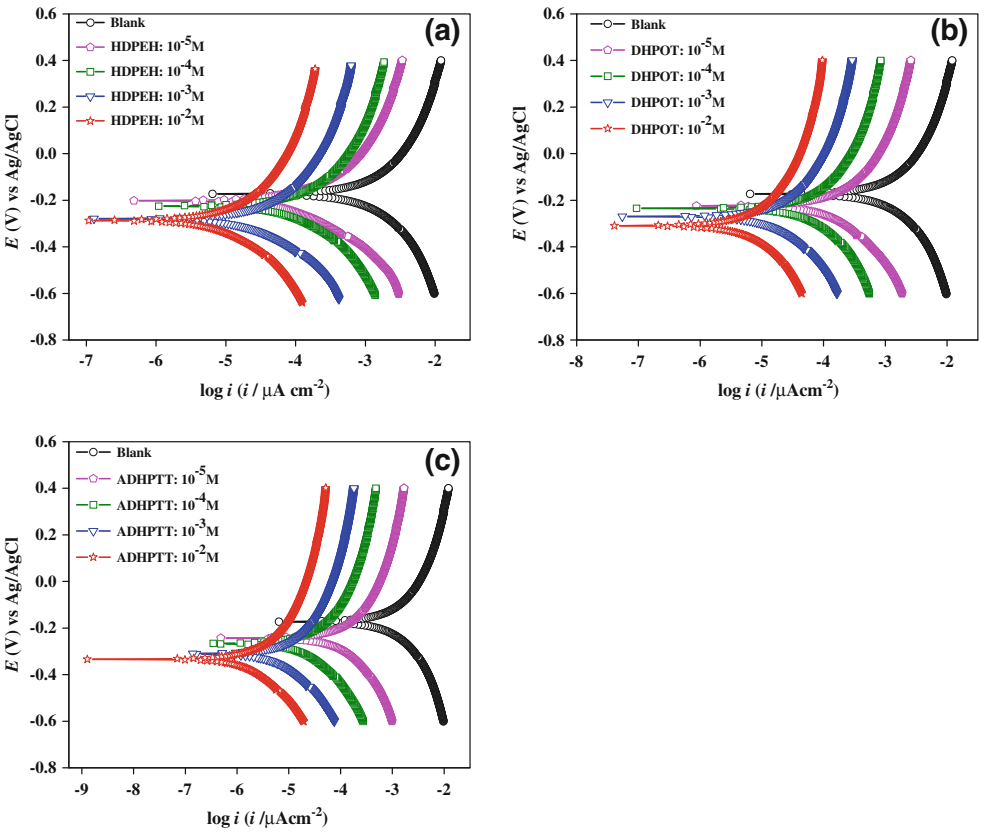

Fig. 2 Potentiodynamic polarisation curves for brass in natural sea water in the absence and presence of various concentrations of **a** HDPEH, **b** DHPOT and **c** ADHPTT

that the investigated organic compounds inhibit the corrosion process. Moreover, as the concentration of piperidine derivatives increases, their inhibiting effect increases. In addition, irrespective of the molecular structure of the piperidine derivatives studied, they appear to have a more pronounced inhibiting effect on both the cathodic and anodic process. The Tafel extrapolation method was used to calculate the corrosion parameters from the polarisation curves in the absence and the presence of different concentrations of inhibitors are given in Table 1. The inhibition efficiency (IE) was calculated using the equation:

$$\mathrm{IE}(\%) = \frac{I_{\mathrm{corr}} - I_{\mathrm{corr(inh)}}}{I_{\mathrm{corr}}} \times 100 \qquad (2)$$

where, I_{corr} and $I_{\mathrm{corr(inh)}}$ are the corrosion current density values without and with inhibitors, respectively. It can be seen that in the absence of inhibitors, the corrosion current density of brass reaches a maximum which indicated the

Table 1 Tafel polarisation parameters for the corrosion of brass in natural sea water in the absence and presence of different concentrations (10^{-5}–10^{-2} M) of HDPEH, DHPOT and ADHPTT

Compound	Concentration (M)	$-E_{\mathrm{corr}}$ (mV)	I_{corr} (μA cm^{-2})	β_c (mV/dec)	β_a mV/dec	CR (mm y^{-1})×10^{-3}	IE (%)
Blank	–	173	2.95	48	56	124	–
HDPEH	10^{-5}	202	1.73	58	86	72	41
	10^{-4}	225	1.24	61	98	53	58
	10^{-3}	280	0.26	72	105	11	91
	10^{-2}	286	0.25	73	106	10	92
DHPOT	10^{-5}	224	1.67	62	89	70	43
	10^{-4}	235	1.19	68	104	50	60
	10^{-3}	309	0.20	78	122	8	93
	10^{-2}	311	0.18	80	123	8	94
ADHPTT	10^{-5}	243	1.61	65	92	67	45
	10^{-4}	266	1.14	71	110	48	61
	10^{-3}	334	0.13	84	125	5	96
	10^{-2}	337	0.12	85	126	5	96

high corrosion rate. However, the presence of HDPEH, DHPOT and ADHPTT results in decrease of corrosion current density. These results showed that the presence of inhibitors in sea water leads to shift in corrosion potential (E_{corr}) values. Small changes in potentials are due to the result of the competition of the anodic and the cathodic inhibiting reactions, and of the metal surface condition. Further, the values of the Tafel coefficients in the presence of the inhibitors significantly change with the inhibitor concentration, which indicates the influence on both the cathodic and anodic reactions. Thus these inhibitors act as mixed type inhibitors for brass in natural sea water [20–22]. For instance, the maximum inhibition efficiencies obtained for HDPEH, DHPOT and ADHPTT at 10^{-2} M concentration was 92, 94 and 96% respectively.

The inhibiting effect could be found in the ability of the chemisorption of organic molecules on the brass surface and protection from corrosion [23, 24]. The highest inhibition efficiency was noticed in the presence of ADHPTT due to the presence of sulphur, nitrogen and oxygen atoms besides phenyl rings. The optimum concentration of piperidine derivatives from the polarisation curves is found to be 10^{-3} M. All the inhibitors exhibited decrease in corrosion rate with increase in concentration. The order of their inhibition efficiency is ADHPTT>DHPOT and>HDPEH.

Electrochemical impedance spectroscopic measurements

The Nyquist plot for brass specimen recorded at the open-circuit potential after 1 h immersion in natural sea water containing various concentrations of piperidine derivatives are shown in Fig. 3 and the corresponding Bode phase angle diagrams are presented in Fig. 4. All the spectra exhibit a capacitive behaviour in the whole frequency domain. The addition of HDPEH, DHPOT and ADHPTT to the aggressive solution leads to increase in impedance values. The equivalent circuit in Fig.4 has been proposed for brass in sea water with piperidine derivatives [25–27]. In the presence of the piperidine derivatives, three capacitive loops, though poorly separated from each other, are necessary for computer fitting of experimental data with an electrical equivalent circuit (Fig. 5b), however only two time constants are observed for blank (Fig. 5a).

The calculated parameters obtained from equivalent circuit fitting analysis with and without inhibitor in sea water are given in Table 2. The impedance response typically reflects a distribution of reactivity that is commonly represented in equivalent electrical circuits as a constant phase element (CPE).The impedance can be expressed in terms of a CPE as

$$Z(\omega) = R + \frac{1}{(j\omega)^n C} \quad \text{Where} \quad 0 < n \leq 1 \tag{3}$$

where, Z is the impedance, ω is the angular frequency, R is the resistance, C is the capacitance and n is a factor that satisfies the condition $0 \leq n \leq 1$, which indicates how far (0), or how close (1), the interface is from being treated as an ideal capacitor. The parameters n and C are independent of frequency. When $n=1$, C has unit of a capacitance, i.e., F/cm^2, and represents the capacity of the interface. Independent of the cause of CPE behaviour, the phase angle associated with a CPE is independent of frequency.

It can be seen from the table that all three capacitances decrease with increase in concentration of inhibitors. The oxide film becomes slightly thicker (C_f), then the double layer capacitance (C_{dl}) decreases, and the amount available for the oxidation–reduction process (C_F) too decreases [28]. The film resistance R_f increases with increase in the concentration of the piperidine derivatives, whereas the C_f values decreases proving that the surface film formed in presence of the investigated organic compounds is probably thicker, less permeable and highly adsorbed [29]. The increase in R_f and the decrease in C_f can be related to the adsorption of inhibitor on the brass surface. The charge transfer resistance (R_{ct}) increases and the double layer capacitance (C_{dl}) decreases on increase in concentration of the inhibitors indicating the decreased corrosion rate and increased corrosion inhibition, which is due to the adsorption of the inhibitor at the metal surface causing a change in the double layer structure.

The value of faradaic resistance (R_F) indicated the stability of surface film on the metal surface tends to increase with increase in concentration of the studied inhibitors. In the presence of inhibitors, the n_F values are found to be near 1, which shows that the films formed acts as an insulator. Therefore R_F is based on both the anodic process corresponding to the metal dissolution and/or the surface film formation, and the cathodic process.

The IE of the piperidine derivatives was calculated from the polarisation resistance values obtained from electrochemical impedance spectroscopy (EIS) measurements, according to the following equation:

$$\mathrm{IE}(\%) = \frac{R_{p(inh)} - R_p}{R_{p(inh)}} \times 100 \tag{4}$$

where, $R_{P(inh)}$ and R_P are polarisation resistance in the presence and absence of inhibitors in electrolytes respectively [30, 31]. The inhibition efficiency increases with increase in concentration and maximum inhibition efficiency was obtained for ADHPT. The percent IE calculated from EIS shows the same trend as those estimated from polarisation measurements, i.e. polarisation measurements and EIS study complement each other well.

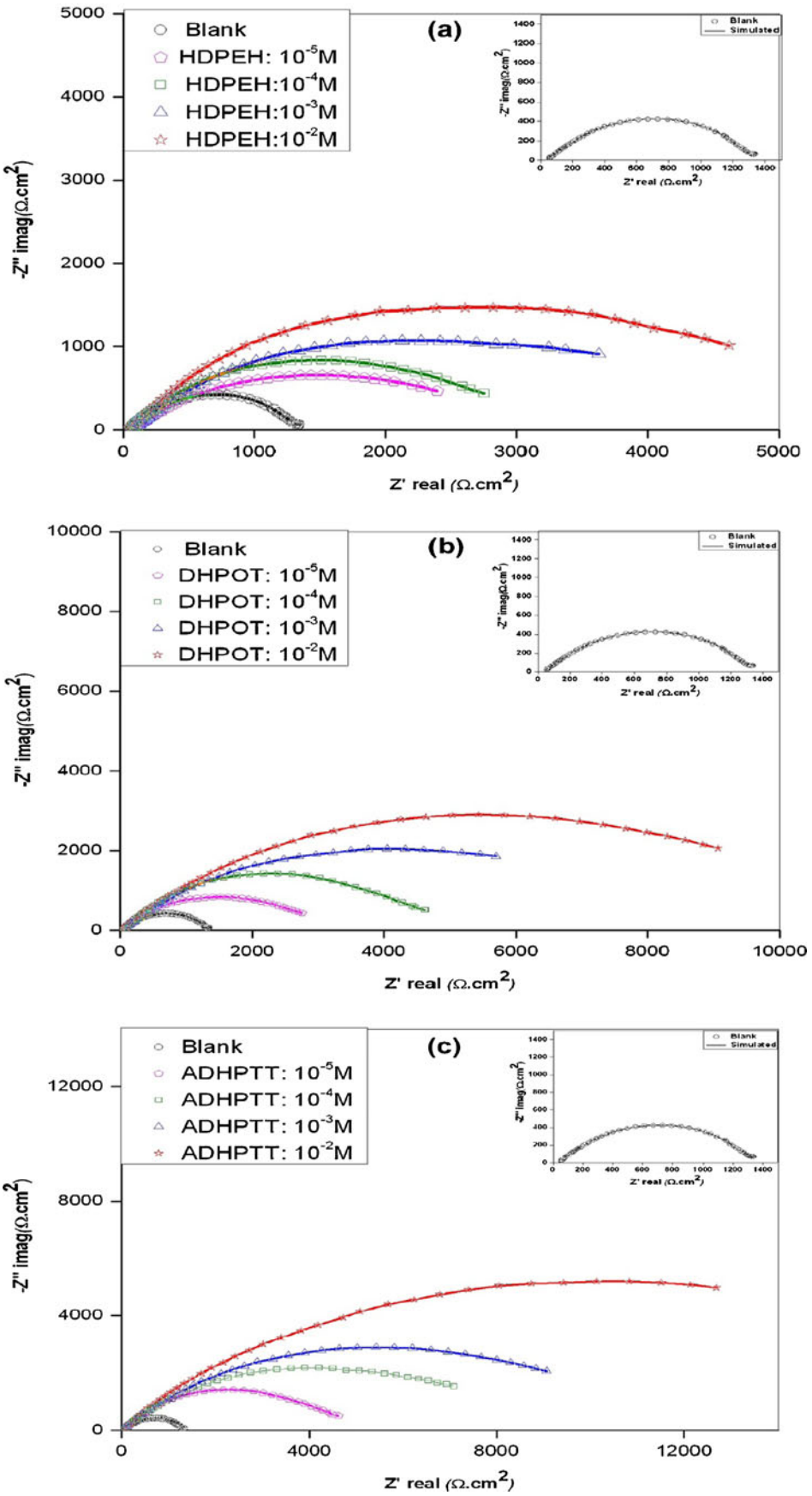

Fig. 3 Nyquist plots of brass electrode in natural sea water in the absence and presence of different concentrations of piperidine derivatives. **a** HDPEH, **b** DHPOT and **c** ADHPTT

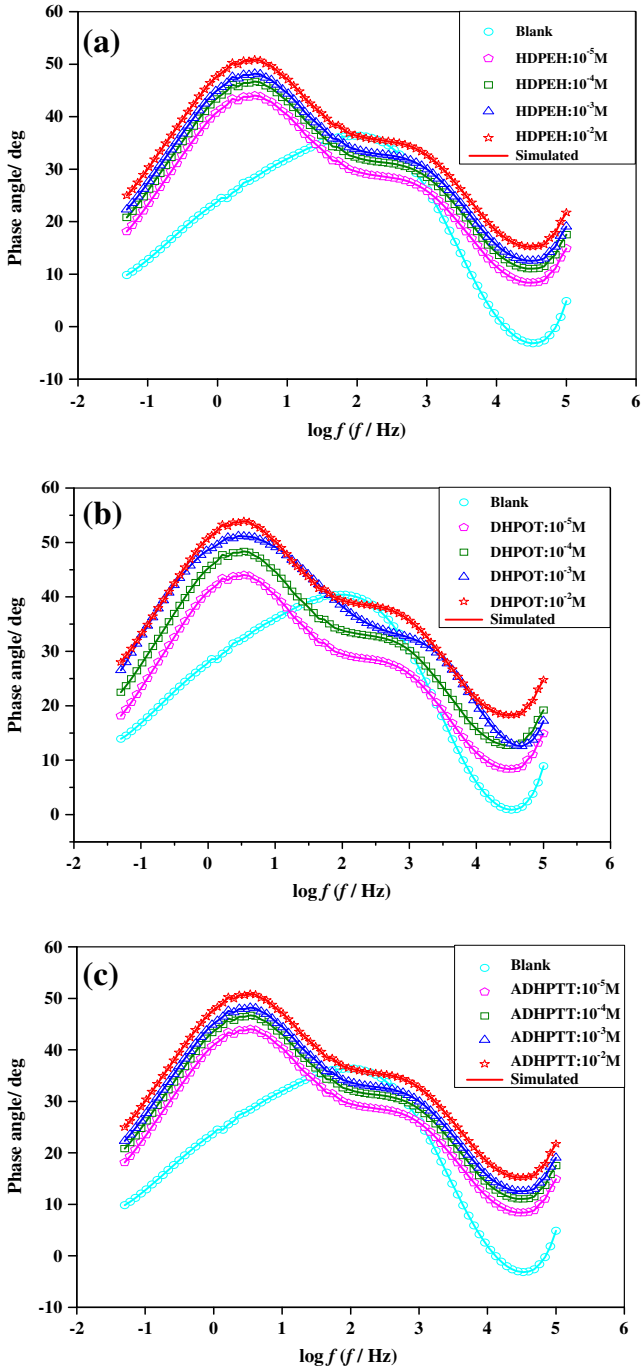

Fig. 4 Bode phase angle diagram of **a** HDPEH, **b** DHPOT and **c** ADHPTT

Effect of temperature

The effect of temperature on the rate of dissolution of brass in natural sea water containing optimum concentration (10^{-3} M) of the investigated inhibitors was tested by potentiodynamic polarisation method over a temperature range from 303 to 343 K and is shown in Fig. 6. The corrosion parameters and inhibition efficiencies exhibited at these temperatures are given in Table 3. The results revealed that on increasing the temperature there is an increase in corrosion current density as well as corrosion rate for uninhibited and inhibited solutions. The dependence of the corrosion rate on temperature can be expressed by the Arrhenius equation, since the corrosion reaction can be regarded as an Arrhenius type process. The activation parameters can be calculated using the Arrhenius equation:

$$I_{\text{corr}} = A\exp(-E_a/RT) \quad (5)$$

where the pre-exponential factor A is the adsorption constant and E_a is the activation energy of the corrosion process. Plotting the natural logarithm of the corrosion current density against $1/T$, the activation energies in the absence and presence of optimum concentration of inhibitors were calculated from the slope. Figure 7 presents the Arrhenius plots for brass in natural sea water without and with addition of 10^{-3} M concentration of HDPEH, DHPOT and ADHPTT at differnt temperatures. For instance, the activation energy for the blank was found to be 11.5 kJ mol^{-1}. However, in the presence of HDPEH, DHPOT and ADHPTT, the activation energies were 57.4, 59.5 and 67.2 kJ mol^{-1}, respectively.

It is clear that the activation energy values obtained in the presence of inhibitors are higher than that obtained in the absence of inhibitor, indicating that the addition of inhibitors enhances corrosion resistance of brass [32]. The higher E_a value for the brass in the inhibited solution can be correlated with the increased stability of the film formed, which enhances the activation energy of the corrosion process. Generally, an increase in temperature usually accelerates corrosive processes, giving rise to higher metal dissolution rates and a possible shift of the adsorption–desorption equilibrium towards desorption. This, as well as roughening of the metal surface as a result of enhanced corrosion, may also reduce the adsorption ability of the inhibitor on the metal surface. The increase in solution temperature slightly shifts E_{corr} in the positive direction and enhances both cathodic and anodic current densities. The decrease in inhibition efficiency with increasing temperature may be due to the increase in desorption of inhibitors followed by dissolution of zinc and copper [33].

Inductively coupled plasma atomic emission spectroscopic studies

The concentrations of copper and zinc in solutions containing 10^{-3} M of the piperidine derivatives after the polarisation measurements were determined from ICP-AES analysis. The dezincification (z) factor for brass in the absence and presence of 10^{-3} M of HDPEH, DHPOT and ADHPTT in natural sea water was calculated from the ICP-AES data and the results of the accelerated leaching study are presented in Table 4. It is observed that the amount of

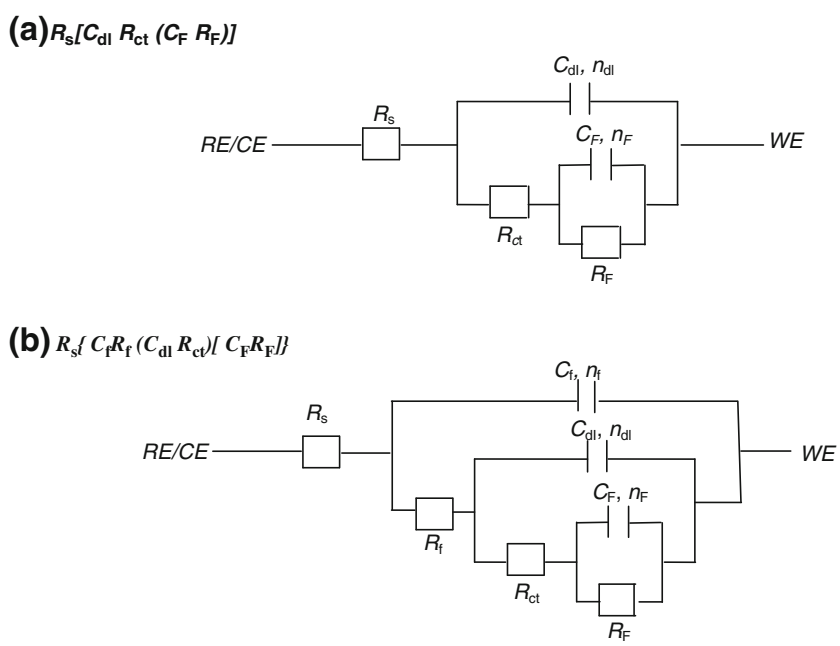

Fig. 5 The equivalent electrical circuits used for computer fitting of the experimental data for the brass electrode in natural sea water **a** in the absence, **b** in the presence of HDPEH, DHPOT and ADHPTT

Zn and Cu leached out from the brass into the electrolyte was significant. However, the presence of inhibitors viz., HDPEH, DHPOT and ADHPTT exhibited a minimal leach out of metal ions. This can be attributed mainly to the formation of the stable film that inhibits metal dissolution by forming a barrier layer between the metal and the environment, thus preventing the bare metal from leaching. It is known that dezincification was much higher in the absence of inhibitors, while they were much lower in the presence of 10^{-3} M concentration of HDPEH, DHPOT and

Table 2 Electrochemical parameter values for brass corrosion calculated by non-linear least square regression of the impedance data using the electrical equivalent circuits

Inhibitor concentration (M)	R_s (kΩ cm^2)	R_f (kΩ cm^2)	C_f (μF cm^{-2})	n_f	R_{ct} (kΩ cm^2)	C_{dl} (μF cm^{-2})	n_{dl}	R_F (kΩ cm^2)	C_F (μF cm^{-2})	n_F	IE (%)
Blank	0.04	–	–	–	1.27	144.3	0.57	1.73	35.5	0.60	–
HDPEH											
10^{-5}	0.11	1.26	15.8	0.72	1.88	18.4	0.71	1.97	13.3	0.71	41
10^{-4}	0.17	1.74	9.2	0.82	2.65	9.9	0.82	2.72	8.3	0.82	58
10^{-3}	0.23	8.88	3.5	0.92	12.23	3.7	0.92	12.29	2.9	0.92	91
10^{-2}	0.23	9.09	3.4	0.92	12.52	3.5	0.92	12.61	2.9	0.92	91
DHPOT											
10^{-5}	0.14	1.33	13.1	0.74	1.95	16.6	0.72	2.03	11.3	0.73	43
10^{-4}	0.21	1.86	7.4	0.84	2.77	7.8	0.84	2.83	6.6	0.84	60
10^{-3}	0.27	11.20	3.0	0.95	15.77	3.2	0.93	16.99	2.4	0.94	93
10^{-2}	0.27	11.88	2.9	0.95	16.99	3.1	0.93	17.93	2.4	0.95	94
ADHPTT											
10^{-5}	0.16	1.42	11.4	0.76	2.01	14.6	0.75	2.12	9.3	0.75	46
10^{-4}	0.26	1.99	5.5	0.87	2.87	5.7	0.86	2.95	4.1	0.85	62
10^{-3}	0.35	16.58	2.5	0.97	22.62	2.7	0.96	23.61	1.9	0.96	96
10^{-2}	0.38	18.98	2.4	0.97	25.88	2.6	0.96	27.97	1.9	0.96	96

$R_{p(inh)}=R_f+R_{ct}+R_F$ and $R_P=R_{ct}+R_F$

R_S electrolyte resistance; R_{ct} charge transfer resistance; C_{dl} charge transfer capacitance; R_F Faradic resistance; C_F Faradic capacitance; R_f film resistance; C_f capacitance due to surface film; n_f, n_{dl} and n_F coefficients representing the depressed characteristic of the three capacitive loops

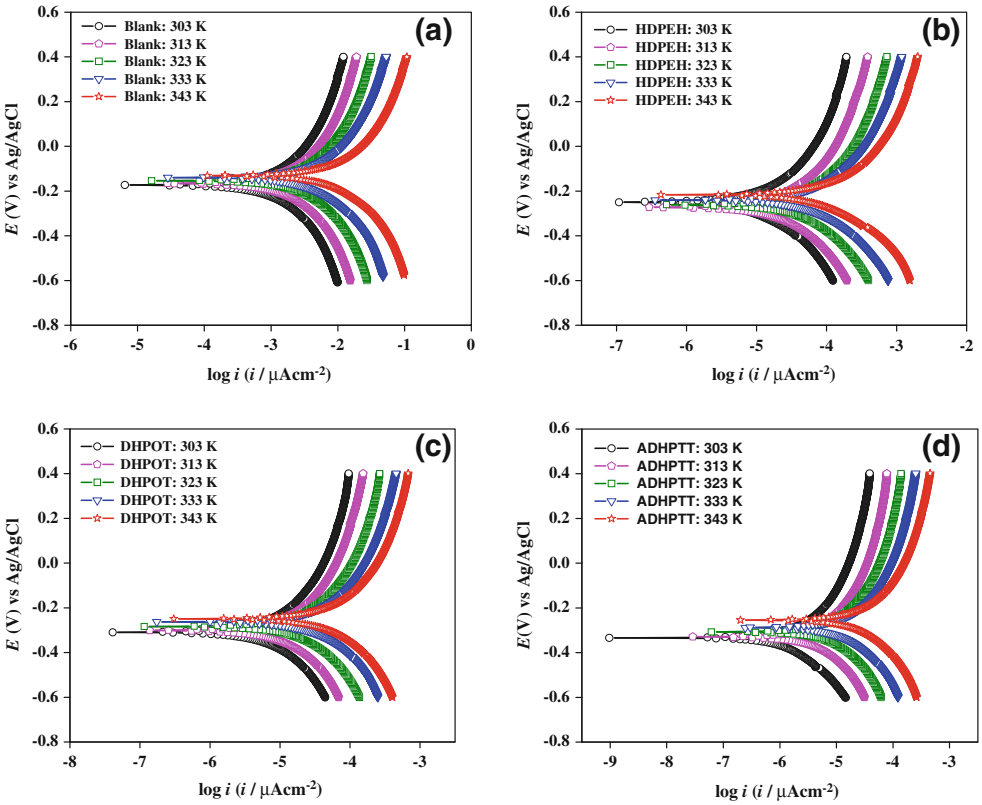

Fig. 6 Effect of temperature on the potentiodynamic polarisation curves for brass in natural sea water in **a** the absence and presence of optimum concentrations (10^{-3} M) of **b** HDPEH, **c** DHPOT and **d** ADHPTT

Table 3 Effect of temperature on the Tafel polarisation parameters for the corrosion of brass in natural sea water in the absence and presence of optimum concentration (10^{-3} M) of HDPEH, DHPOT and ADHPTT

Compound	Temperature (K)	$-E_{corr}$ (mV)	I_{corr} (μA cm^{-2})	β_c mV/dec	β_a mV/dec	*CR* (mm y^{-1})×10^{-3}	IE (%)
Blank	303	173	2.95	48	56	124	–
	313	165	3.42	43	51	138	–
	323	154	3.94	37	45	148	–
	333	140	4.45	30	38	160	–
	343	131	5.15	22	30	174	–
HDPEH	303	284	0.26	72	105	11	91
	313	274	0.65	70	103	27	81
	323	261	1.38	67	99	52	65
	333	240	2.42	63	94	87	46
	343	216	4.10	58	88	139	20
DHPOT	303	309	0.20	78	122	8	93
	313	301	0.61	74	109	24	82
	323	284	1.21	71	107	45	69
	333	263	2.17	69	101	78	51
	343	239	3.67	64	96	125	29
ADHPTT	303	334	0.13	84	125	5	96
	313	329	0.49	78	118	20	86
	323	307	1.04	75	112	39	74
	333	289	1.88	73	108	68	58
	343	255	3.26	71	102	110	37

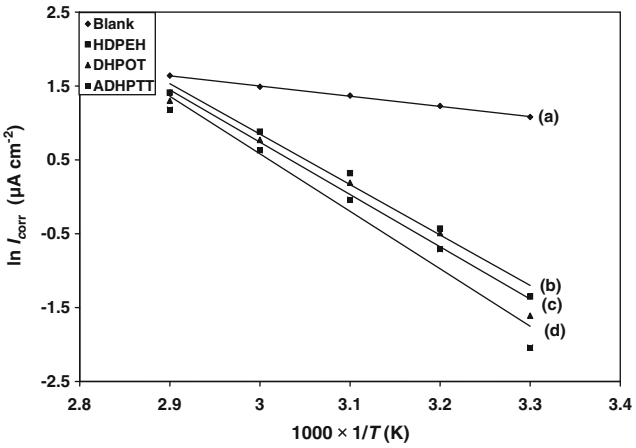

Fig. 7 Arrhenius slopes calculated from corrosion current density for brass in the natural sea water **a** blank and presence of **b** HDPEH, **c** DHPOT and **d** ADHPTT

ADHPTT. The percent inhibition efficiency against the dissolution of zinc was correspondingly higher as compared to the dissolution of copper. This suggests that the piperidine derivatives efficiently prevent the dezincification of brass in natural sea water, which is also reflected in the values of the dezincification factor.

SEM–EDX investigations

Both SEM and EDX experiments were carried out in order to verify if the molecules of piperidine derivatives are in fact adsorbed on brass surface. The SEM micrograph obtained for the brass surface in the absence and presence of optimum concentration of the studied piperidine derivatives in natural sea water are shown in Fig. 8. The brass surface in the absence of inhibitors exhibited a highly corroded surface with pits and cracks (Fig. 8a). This is due to the attack of brass surface with aggressive chloride ions in natural sea water. However, in the presence of HDPEH, DHPOT and ADHPTT which revealed that the brass surface can be observed with a thin layer of the inhibitor molecules, giving protection against corrosion. The inhibited metal surface is smoother than the uninhibited surface indicating the presence of a protective layer of adsorbed inhibitor preventing chloride attack in natural sea water (Fig. 8b). This is due to the formation of copper and zinc complexes of HDPEH, DHPOT and ADHPTT that protect the brass surface against corrosion. The formation of the complex with inhibitors on the brass surface has higher stability and low permeability in aggressive solution than uninhibited brass surface. So they show much better film properties, which seemed to provide some corrosion protection to the metal beneath them by restricting the mass transfer of reactants and products between the bulk solution and the metal surface.

EDX spectra were used to determine the elements present on the brass surface before and after exposure to the inhibitor solution. Figure 9 (a–d) presents the EDX spectra for the samples in the absence and presence of optimal concentrations of studied piperidine derivatives. In the absence of inhibitor molecules, the EDX spectra confirm the existence of chlorine and oxygen along with copper and zinc due to the formation of Cu_2O and $CuCl_2^-$ complex [34]. However, in the presence of the optimum concentrations of the HDPEH, DHPOT and ADHPTT inhibitors, nitrogen, oxygen and sulphur atoms are found to be present and coordinated with the brass surface, thus forming the complexes of the studied inhibitors on the brass surface. This indicates that the studied inhibitor molecules are adsorbed on the brass surface, thus protecting the brass surface against corrosion.

Mechanism of corrosion inhibition

The adsorption of HDPEH, DHPOT and ADHPTT can occur directly on the basis of donor acceptor interactions between π-electrons and N, O and S atoms of the neutral species as well as π-electrons of cationic species and the vacant *d*-orbital of copper and zinc [35, 36]. It has been reported that the adsorption of the heterocyclic compounds occurs with the aromatic rings sometimes parallel but mostly normal to the metal surface. Owing to the adsorption of the inhibitor onto the surface of the brass, a thin film is formed on the brass to retard the corrosion. Thus, in this case, HDPEH, DHPOT and ADHPTT worked as the filming inhibitor to control the corrosion rate. Instead of reacting with or removing an active corrosive species, the filming inhibitors function by strong adsorption and decrease the attack by creating a barrier between the metal

Table 4 Effect of HDPEH, DHPOT and ADHPTT on the dezincification of brass in natural sea water at optimum concentrations (10^{-3} M) for all inhibitors

Inhibitors	Solution analysis		Dezincification factor (*z*)	Percent inhibition	
	Cu/10^{-8} M	Zn/10^{-8} M		Cu	Zn
Blank	74	1,725	43	–	–
HDPEH	8	124	19	89	93
DHPOT	6	101	17	92	94
ADHPTT	4	27	12	95	98

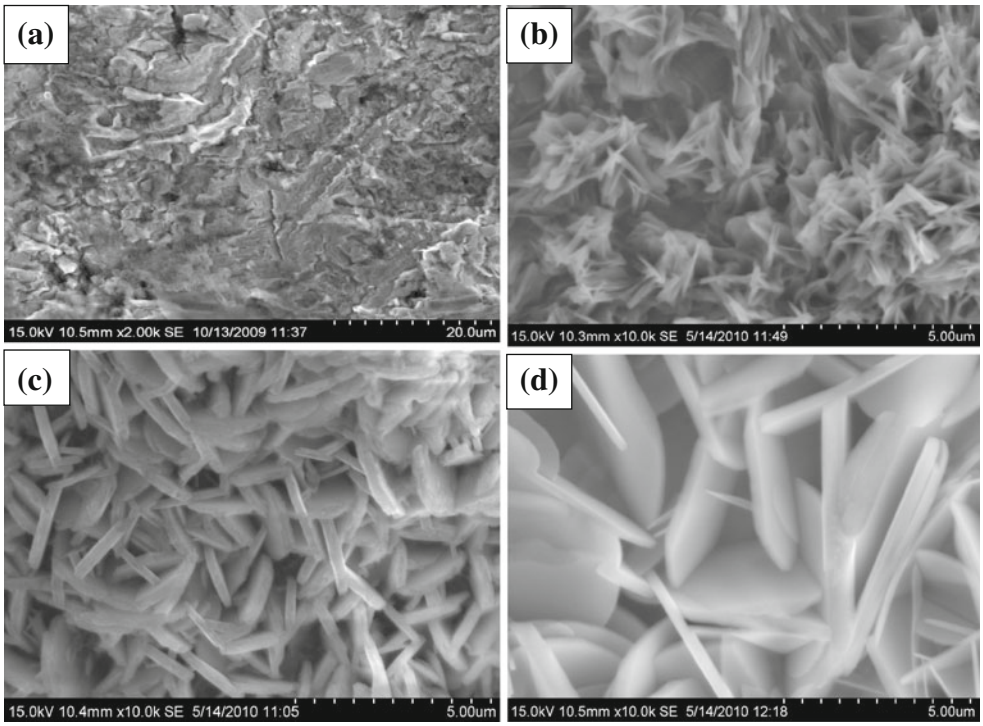

Fig. 8 SEM images of brass without and with inhibitor **a** blank, **b** HDPEH, **c** DHPOT and **d** ADHPTT

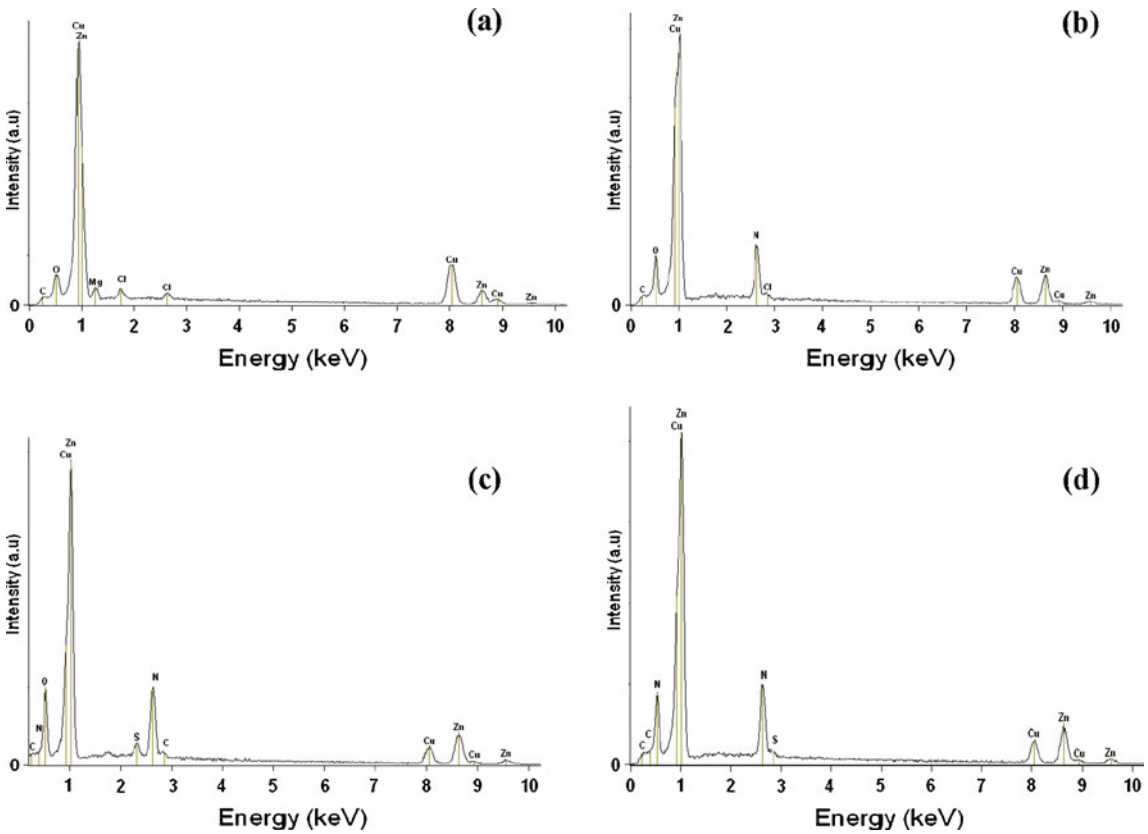

Fig. 9 EDX profile for brass surface **a** blank, **b** HDPEH, **c** DHPOT and **d** ADHPTT

and their environment [37]. The inhibition process of piperidine derivatives could be explained as follows: piperidine is an aromatic compound and it contains two phenyl groups and one hydrazide group around the aromatic ring. In addition to this, HDPEH contains ethanoic acid hydrazide at the N atom of the piperidine derivatives, 1, 3, 4-oxadiazole-2-thione group is attached to the DHPOT and 1, 2, 4-triazole-3-thiol is attached to the ADHPTT (Fig. 1). Thus, the adsorption of piperidine derivatives onto the surface of the brass may take place through all these functional groups. The simultaneous adsorption of the three functional groups forces the piperidine derivatives molecule to be horizontally oriented at the surface of the brass.

It is generally assumed that the adsorption of inhibitor at the metal/solution interface is the mechanism of inhibition through electrostatic attraction between the charged molecules and charged metal. Among the compounds investigated in the present study, ADHPTT has been found to give an excellent inhibition due to the presence of additional electron donating groups (such as SH and NH_2) on the piperidine derivatives, which increase the electron density on the nitrogen, oxygen and sulphur containing groups. This leads to the strong adsorption of ADHPTT on the metal surface thereby resulting in high inhibition efficiency.

Conclusions

Polarisation studies revealed that the compounds HDPEH, DHPOT and ADHPTT show good inhibiting properties that increase with inhibitor concentration. EIS measurements indicated that the inhibitors hinder the corrosion process due to the increase of charge transfer resistance, film resistance and faradaic resistance related to the stabilisation of adsorbed films. SEM and EDX analysis showed that a film of inhibitor was formed on the brass surface. The film inhibited the growth of oxides of copper and zinc. ICP-AES analysis revealed that the investigated inhibitors effectively control the dezincification of brass. Hence, the ADHPTT can be used to protect the brass used in cooling water systems.

Acknowledgement One of the authors, X. Joseph Raj, acknowledges the University Grant Commission (UGC), New Delhi for financial assistance.

References

1. El Warraky A, El Shayeb HA, Sherif EM (2004) Anti-Corros Methods Mater 51:52–61
2. Sherif EM, Erasmus RM, Comins JD (2007) J Colloid Interface Sci 309:470–477
3. Quartarone G, Moretti G, Bellomi T (1998) Corrosion 54:606–618
4. Qu Q, Jiang S, Bai W, Li L (2007) Electrochim Acta 52:6811–6820
5. Quraishi MA, Sardar R (2002) Corrosion 58:748–755
6. Zor S, Doğan P, Yazici B (2005) Corros Sci 47:2700–2710
7. Selvi ST, Raman V, Rajendran N (2003) J Appl Electrochem 33:1175–1182
8. Mansfeld F, Smith T (1973) Corrosion 29:105–107
9. Elmorsi MA, Hassanien AM (1999) Corros Sci 41:2337–2352
10. Abd El-Maksoud SA (2004) J Electroanal Chem 565:321–328
11. Christy AG, Lowe A, Otieno-Alego V, Stoll M, Webster RD (2004) J Appl Electrochem 34:225–233
12. Bastidas JM, Pinilla P, Cano E, Polo JL, Miguel S (2003) Corros Sci 45:427–449
13. Rodrı'guez-Valdez LM, Martınez-Villafane A, Glossman-Mitnik D (2005) J Mol Struct THEOCHEM 713:65–70
14. Bouklah M, Benchat N, Hammouti B, Aouniti A, Kertit S (2006) Mater Lett 60:1901–1905
15. Bentiss F, Traisnel M, Lagrene M (2001) J Appl Electrochem 31:41–48
16. Ravichandrana R, Rajendran N (2004) Appl Surf Sci 241:449–458
17. Khaled KF, Amin MA (2008) J Appl Electrochem 38:1609–1621
18. Ravichandran R, Nanjundan S, Rajendran N (2004) J Appl Electrochem 34:1171–1176
19. Ravichandran R, Nanjundan S, Rajendran N (2004) Appl Surf Sci 236:241–250
20. Fouda AS, Mostafa HA, El-Abbasy HM (2010) J Appl Electrochem 40:163–173
21. Hosseini MG, Ehteshamazadeh M, Shahrabi T (2007) Electrochim Acta 495:3680–3685
22. Zhang Z, Chen S, Li Y, Li S, Wanga L (2009) Corros Sci 51:291–300
23. Sherif ESM (2006) Appl Surf Sci 252:8615–8623
24. Sherif ESM, Park SM (2006) Corros Sci 48:4065–4079
25. Otmacic Curkovic H, Stupnisek-Lisac E, Takenouti H (2009) Corros Sci 51:2342–2348
26. Benmessaoud M, Es-salah K, Hajjaji N, Takenouti H, Shriri A, Ebentouhami M (2007) Corros Sci 49:3880–3888
27. Otmacic Curkovic H, Stupnisek-Lisac E, Takenouti H (2010) Corros Sci 52:398–405
28. Rahmouni K, Hajjaji N, Keddam M, Srhiri A, Takenouti H (2007) Electrochim Acta 52:7519–7528
29. Rahmouni K, Keddam M, Srhiri A, Takenouti H (2005) Corros Sci 47:3249–3266
30. Trachli B, Keddam M, Takenouti H, Srhiri A (2002) Corros Sci 44:997–1008
31. Varvara S, Muresan LM, Rahmouni K, Takenouti H (2008) Corros Sci 50:2596–2604
32. Fouda AS, Al-Sawary AA, Ahmed FSh, El-Abbasy HM (2009) Corros Sci 51:485
33. Mohamed Amin A (2006) J Appl Electrochem 36:215–226
34. Hegazy HS, Ashour EA, Ateya BG (2001) J Appl Electrochem 31:1261–1265
35. Cicileo GP, Rosales BM, Varela FE, Vilche JR (1999) Corros Sci 41:1359–1375
36. Saleh MM (2006) Mater Chem Phys 98:83–89
37. Al-Juhni AA, Newby BZ (2006) Prog Org Coat 56:135–145